Research Article | Vol. 25, No. 18 | 4 Sep 2017 | OPTICS EXPRESS 21025
Optics EXPRESS

Self-selection mechanism of Fabry-Pérot micro/nanoscale wire cavity for single-mode lasing

YUE YANG,[1,4] HUA ZONG,[1,4] CHUANG MA,[2] TIANTIAN WEI,[1] JUNCHAO LI,[1] JIANG ZHANG,[3] MO LI,[3] CAOFENG PAN,[2] AND XIAODONG HU[1,*]

[1]*State Key Laboratory for Artificial Microstructure and Mesoscopic Physics, School of Physics, Peking University, Beijing 100871, China*
[2]*Beijing Institute of Nanoenergy and Nanosystems, Chinese Academy of Sciences, Beijing 100083, China*
[3]*Microsystem and Terahertz Research Center, CAEP, Shuangliu, Chengdu 610200, Si-chuan, China*
[4]*These authors contributed equally to this work*
[*]*huxd@pku.edu.cn*

Abstract: Developing micro/nanoscale wire (MNW) lasers with single-mode operation is critical for realizing their practical applications, however, most reported MNW lasers operate in multi-modes, because lacking of mode selection mechanisms. In this work, a simple and direct way to realize stable, single-mode MNW laser without complicated micro/nano-manipulation was demonstrated. We have found and proved that the position of the active region plays a key role in determining the lasing mode of MNW lasers, which can be used to realize single-mode lasing in MNWs. We propose self-selection mechanism of Fabry-Pérot MNW cavity for single-mode lasing due to location-dependent field distribution in MNWs, which is characterized by suppressing the multiple longitudinal mode oscillation of the MNW laser. GaN MNW lasers with different lengths and diameters have been fabricated, verifying the self-selection mechanism of the cavity experimentally. Moreover, we demonstrate the single-mode, room temperature optically pumped MNW laser with an extremely low threshold (~40 kW/cm^2) in condition of appropriate cavity length, opening an opportunity to realize stable single-mode, low-threshold MNW laser for easy integration in constructing micro/nanoscale photonic and optoelectronic circuits and devices.

OCIS codes: (120.2230) Fabry-Perot; (140.3570) Lasers, single-mode; (160.6000) Semiconductor materials.

References and links

1. R. X. Yan, D. Gargas, and P. D. Yang, "Nanowire photonics," Nat. Photonics **3**(10), 569–576 (2009).
2. B. Janjua, H. D. Sun, C. Zhao, D. H. Anjum, D. Priante, A. A. Alhamoud, F. Wu, X. H. Li, A. M. Albadri, A. Y. Alyamani, M. M. El-Desouki, T. K. Ng, and B. S. Ooi, "Droop-free AlxGa1-xN/AlyGa1-yN quantum-disks-in-nanowires ultraviolet LED emitting at 337 nm on metal/silicon substrates," Opt. Express **25**(2), 1381–1390 (2017).
3. M. H. Huang, S. Mao, H. Feick, H. Yan, Y. Wu, H. Kind, E. Weber, R. Russo, and P. Yang, "Room-Temperature Ultraviolet Nanowire Nanolasers," Science **292**(5523), 1897–1899 (2001).
4. I. Giuntoni, L. Geelhaar, J. Bruns, and H. Riechert, "Light coupling between vertical III-As nanowires and planar Si photonic waveguides for the monolithic integration of active optoelectronic devices on a Si platform," Opt. Express **24**(16), 18417–18427 (2016).
5. Y. Xia, P. Yang, Y. Sun, Y. Wu, B. Mayers, B. Gates, Y. Yin, F. Kim, and H. Yan, "One-dimensional nanostructures: synthesis, characterization, and applications," Adv. Mater. **15**(5), 353–389 (2003).
6. H. Zhu, Y. Fu, F. Meng, X. Wu, Z. Gong, Q. Ding, M. V. Gustafsson, M. T. Trinh, S. Jin, and X. Y. Zhu, "Lead halide perovskite nanowire lasers with low lasing thresholds and high quality factors," Nat. Mater. **14**(6), 636–642 (2015).
7. D. Saxena, S. Mokkapati, P. Parkinson, N. Jiang, Q. Gao, H. H. Tan, and C. Jagadish, "Optically pumped room-temperature GaAs nanowire lasers," Nat. Photonics **7**(12), 963–968 (2013).
8. S. Arafin, X. H. Liu, and Z. T. Mi, "Review of recent progress of III-nitride nanowire lasers," J. Nanophotonics **7**(1), 074599 (2013).
9. A. Dobrovolsky, J. E. Stehr, S. Sukrittanon, Y. Kuang, C. W. Tu, W. M. M. Chen, and I. A. Buyanova, "Fabry-Perot Microcavity Modes in Single GaP/GaNP Core/Shell Nanowires," Small **11**(47), 6331–6337 (2015).

#301234 https://doi.org/10.1364/OE.25.021025
Journal © 2017 Received 3 Jul 2017; revised 11 Aug 2017; accepted 11 Aug 2017; published 21 Aug 2017

Optics EXPRESS

10. B. E. A. Saleh and M. C. Teich, *Fundamentals of Photonics* (Wiley, 2007), Chapter 14.
11. Q. Li, J. B. Wright, W. W. Chow, T. S. Luk, I. Brener, L. F. Lester, and G. T. Wang, "Single-mode GaN nanowire lasers," Opt. Express **20**(16), 17873–17879 (2012).
12. L. Chen and E. Towe, "Nanowire lasers with distributed-Bragg-reflector mirrors," Appl. Phys. Lett. **89**(5), 053125 (2006).
13. J. B. Wright, S. Campione, S. Liu, J. A. Martinez, H. W. Xu, T. S. Luk, Q. M. Li, G. T. Wang, B. S. Swartzentruber, L. F. Lester, and I. Brener, "Distributed feedback gallium nitride nanowire lasers," Appl. Phys. Lett. **104**(4), 041107 (2014).
14. A. Fu, H. Gao, P. Petrov, and P. Yang, "Widely Tunable Distributed Bragg Reflectors Integrated into Nanowire Waveguides," Nano Lett. **15**(10), 6909–6913 (2015).
15. Y. Xiao, C. Meng, P. Wang, Y. Ye, H. Yu, S. Wang, F. Gu, L. Dai, and L. Tong, "Single-nanowire single-mode laser," Nano Lett. **11**(3), 1122–1126 (2011).
16. H. Gao, A. Fu, S. C. Andrews, and P. Yang, "Cleaved-coupled nanowire lasers," Proc. Natl. Acad. Sci. U.S.A. **110**(3), 865–869 (2013).
17. Y. Xiao, C. Meng, X. Q. Wu, and L. M. Tong, "Single mode lasing in coupled nanowires," Appl. Phys. Lett. **99**(2), 023109 (2011).
18. A. Dodabalapur, L. J. Rothberg, R. H. Jordan, T. M. Miller, R. E. Slusher, and J. M. Phillips, "Physics and applications of organic microcavity light emitting diodes," J. Appl. Phys. **80**(12), 6954–6964 (1996).
19. X. W. Liu, P. F. Xu, Y. P. Wu, Z. Y. Yang, C. Meng, W. S. Yang, J. B. Li, D. L. Wang, X. Liu, and Q. Yang, "Control, optimization and measurement of parameters of semiconductor nanowires lasers," Nano Energy **14**, 340–354 (2015).
20. M. M. Y. Leung, A. B. Djurišić, and E. H. Li, "Refractive index of InGaN/GaN quantum well," J. Appl. Phys. **84**(11), 6312–6317 (1998).
21. P. M. Coulon, M. Hugues, B. Alloing, E. Beraudo, M. Leroux, and J. Zuniga-Perez, "GaN microwires as optical microcavities: whispering gallery modes Vs Fabry-Perot modes," Opt. Express **20**(17), 18707–18716 (2012).
22. X. Yan, X. Zhang, J. Li, Y. Wu, J. Cui, and X. Ren, "Fabrication and optical properties of GaAs/InGaAs/GaAs nanowire core-multishell quantum well heterostructures," Nanoscale **7**(3), 1110–1115 (2015).
23. C. Couteau, A. Larrue, C. Wilhelm, and C. Soci, "Nanowire lasers," Nanophotonics **4**(1), 90–107 (2015).
24. L. K. van Vugt, B. Zhang, B. Piccione, A. A. Spector, and R. Agarwal, "Size-dependent waveguide dispersion in nanowire optical cavities: slowed light and dispersionless guiding," Nano Lett. **9**(4), 1684–1688 (2009).
25. C. E. Hofmann, F. J. G. de Abajo, and H. A. Atwater, "Enhancing the radiative rate in III-V semiconductor plasmonic core-shell nanowire resonators," Nano Lett. **11**(2), 372–376 (2011).
26. B. R. Bennett, R. A. Soref, and J. A. Del Alamo, "Carrier-induced change in refractive index of InP, GaAs and InGaAsP," IEEE J. Quantum Electron. **26**(1), 113–122 (1990).
27. F. S. Chen, "Optically Induced Change of Refractive Indices in LiNbO3 and LiTaO3," J. Appl. Phys. **40**(8), 3389–3396 (1969).

1. Introduction

Semiconductor micro/nanoscale wire (MNW) lasers have been a hot issue of significant scientific research due to their promises as integratable micro/nanoscale coherent light sources for wide applications including sensing, digitized communications, and signal processing [1–9]. The spectrum purity of the MNW laser becomes an important figure of merit since laser emission at multiple frequencies can lead to temporal pulse broadening and high bit error ratio (BTR) because of group velocity dispersion [10]. Extensive researches have been done to control MNW lasers to oscillate at a single frequency. A possible way to achieve single-mode operation is greatly shortening the lasing cavity path and therefore expanding the free space range (FSR) of the multiple longitude modes, until only one longitude mode left [11]. However, with the low reflectivity of the end facets, such short MNWs are inefficient resonators with significant reduced round-trip gain, resulting in high threshold for lasing action. With this in mind, fabricating distributed-Bragg-reflector (DBR) mirrors or distributed-feedback (DFB) mirrors on a MNW is proposed to obtain single-mode MNW lasers [12–14], but experimentally it is very difficult and inconvenient to fabricate high quality DBR/DFB structures on a single MNW. Another possible approach indicated by the previous studies is to make use of coupled cavities, which can generate a mode selection mechanism by the Vernier effect [15–17]. However, this approach requires complicated micro/nano-manipulation to create a coupling structure and the difficulty of the integration of different coupled cavities is greatly increased.

To realize the practical applications of the MNW lasers and meet the goal of easy integration, in this letter, we demonstrate a simple and direct way to obtain single-mode low-

Optics EXPRESS

threshold MNW lasers without complicated micro/nano-manipulation. We propose self-selection mechanism of Fabry-Pérot MNW laser for single-mode operation, where mode selection is achieved through the location-dependent field distribution in MNWs.

2. Simulation models and methods

Since MNWs typically have diameters comparable to the emission wavelength and a high dielectric constant contrast between the MNW material and the surrounding ambient, spontaneous emission can easily couple into the guided optical modes along the axial direction in the one-dimensional (1D) geometry waveguides which also function as axial Fabry-Pérot (F-P) cavities with tailorable optical modes. Lifetime changes of the emitter in semiconductor MNWs are sensitive to the cavity design and are location-dependent due to the cavity effects. The approximate theoretical emission spectrum for the typical F-P cavity is known as [18]:

$$\left|\mathrm{E}_{\mathrm{c}}(\lambda)\right|^2 = \frac{(1-R_2)[1+R_1+2\sqrt{R_2}\cos(\frac{2\omega z_1}{c})]}{1+R_1R_2-2\sqrt{R_1R_2}\cos(\frac{2\omega L}{c})}\left|E_n(\lambda)\right|^2. \quad (1)$$

where, R_1 and R_2 are the reflectivity of the mirrors at two ends of the wire, respectively, z_1 is the effective distance of the emitting dipole from the mirror with reflectivity R_1, c is the speed of light in vacuum, ω is the frequency, L is the total optical path length of the cavity, and $E_n(\lambda)$ is the free space photoluminescence intensity at emission wavelength λ. Equation (1) demonstrates that the dipole position in the cavity and the dephasing processes significantly influence the electroluminescence intensity of the longitude lasing modes. While in general, the enhancement of the emission intensity along the cavity axis (at the resonance wavelength) has a maximum value when the emitting dipole is located exactly at the antinode of the standing wave. Unlike normal F-P cavity, semiconductor MNWs are 1D structures serving as a waveguide with strong lateral optical confinement as well as a gain media, and therefore the modification of the spontaneous emission (SE) in MNWs shows unique features compared with the three-dimensional (3D) structures [19]. It is important to understand how the lasing action in MNWs is affected by the cavity effect. Meanwhile, with the practical application problems we are facing, a question is put forward: is there a simple and direct way to realize low-threshold single-mode MNW lasers for easy integration at sub-wavelength dimension? In order to solve the above problems, we will start with the research on how the modification of the SE rate in a MNW cavity may affect the output emission, based on the 3D finite-difference time-domain (FDTD) method. Here the simulations were calculated by 3D FDTD solutions tools (Lumerical FDTD Solutions, Inc.).

Optics EXPRESS

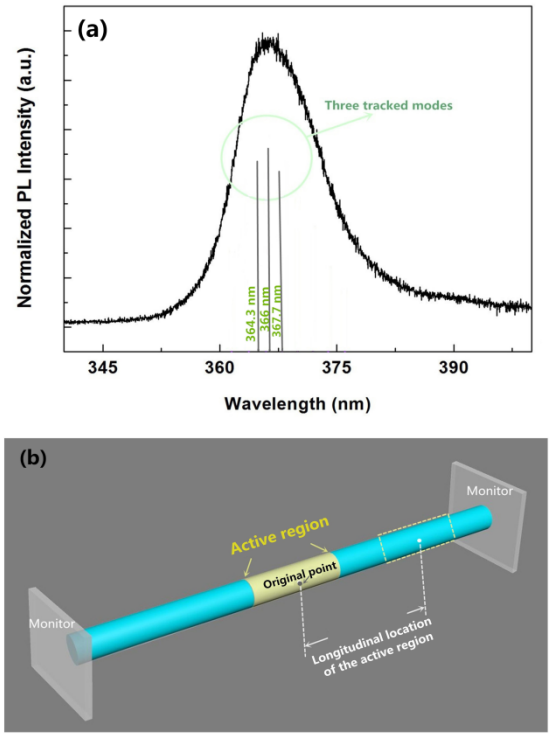

Fig. 1. (a) PL spectrum of a GaN MNW. (b) The computational domain used for calculating the spontaneous emission of the dipole sources by 3D FDTD solutions tools.

Since our synthesized MNWs are about 1.5~3μm in diameter and 30~70 μm in length, we set the length and the diameter of the simulated GaN MNW to be 60 μm and 2 μm, respectively. The wavelength-dependent refractive index of GaN based on experimental measurements is taken from ref [20]. in the simulation. The energy of the waveguide mode in an F-P cavity is given by [21]:

$$E = \frac{1}{2} \times \frac{hc}{L} \times \frac{M}{n}. \tag{2}$$

where c is the speed of light in vacuum, h is the Planck constant, M is the interference order, L is the F-P cavity length, n is the energy dependent refractive index and E is the peak energy. Figure 1(a) shows the photoluminescence (PL) spectrum of a GaN MNW below threshold, and we can determine the positions of the F-P cavity modes for the 60-μm-long, 2-μm-diameter GaN MNW using Eq. (2) (the details on measuring the PL spectrum are shown in the following section). In our simulation, the F-P cavity length (L) is 60 μm, and the energy dependent refractive index of GaN (n) is taken from ref [20]. The calculated results from Eq. (2) validate three axial F-P modes at 364.3, 366 and 367.7 nm in the middle sections of the PL spectrum for the simulated wire geometry with interference order (M) to be 902, 898 and 894, respectively. These three illustrative lasing modes are denoted by sticks below spectrum and circled in green in Fig. 1(a). The behaviors of the spontaneous emission that couples into these three guided modes in the given MNW are to be tracked and studied in the following simulation for illustration.

The computational domain for the 3D FDTD simulation is illustrated in Fig. 1(b). Perfectly matched layers (PMLs) are used to absorb any radiation impinging on the domain boundaries. We have placed a number of dipole sources in the MNW which distributed over a

Optics EXPRESS

range of 15 μm, i.e., the length of the active region is set to be 15 μm (as indicated by the yellow region in Fig. 1(b)). The position at the midpoint between two end facets on the longitudinal axis of the MNW is set to be the original point (which is labeled with gray point in Fig. 1(b)). The active region will move along the axis from the original point and the distance between the original point and the center of the active region is defined as "the longitudinal location of the active region". Since the spontaneous emission from the dipole sources can couple into a radiated or a guided mode (we call the "guided spontaneous emission"), two power flow monitors are placed at two ends of the MNW, which is sufficiently far away from the dipole sources that the optical power of only the truly guided modes is of significance at this end. To make sure the dipole sources can effectively excite the F-P waveguide modes in the FDTD simulation, we have used electric dipoles with orientation parallel to the axis (TM polarized dipoles) and electric dipoles with orientation perpendicular to the axis (TE polarized dipoles) to excite the wire cavity, respectively. However, the spontaneous emission rates couple into the F-P waveguide modes are far weaker under the excitation of TM polarized dipoles, compared to that under the excitation of TE polarized dipoles, indicating that the TM polarized dipoles can't effectively excite the F-P waveguide modes in MNW with such size (1.5~3μm in diameter and 30~70 μm in length). Therefore, we use TE polarized dipoles to excite the axis F-P waveguide modes in MNWs. The active region will move along the axis from its original point in the simulation and the monitors at the far ends will record the spontaneous emission radiated from the dipole sources that couples into the guided modes. It should be noted that as the guided spontaneous emission gives the actual contributions of the spontaneous emission into a resonant lasing mode [22, 23], we will focus on the modification of the guided spontaneous emission rate in the MNW in the following analysis.

3. Simulation results and discussion

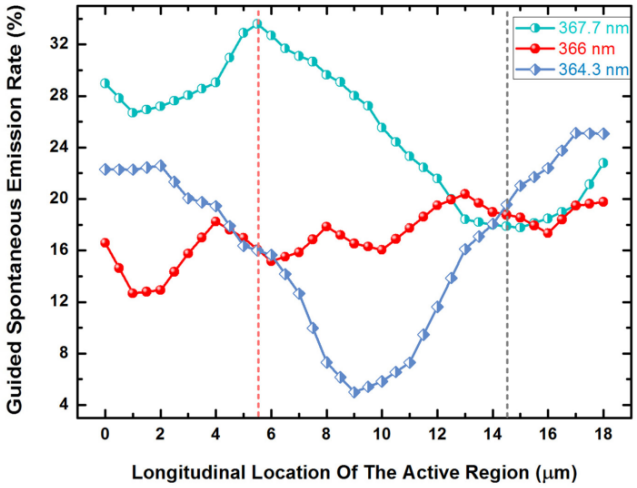

Fig. 2. Normalized guided spontaneous emission rate of dipole sources in a 60-μm-long, 2-μm-diameter GaN MNW at wavelengths of 367.7 nm, 366 nm and 364.3 nm.

Figure 2 shows the normalized SE rate (normalized to the SE rate of the bulk GaN material) that couples into the tracked three lasing modes which are circled in green in Fig. 1(a), as a function of the longitudinal axial location of the active region. Our simulation demonstrates that when the distance between the edge of the active region and the monitor is greater than 4 μm, the radiation from dipoles couples into radiated modes that is recorded by the monitor is nearly 0, therefore the monitor can only capture the guided modes in our simulation. Figure 2 illustrates that the SE rate for each wavelength is enhanced at certain positions with the use of

Optics EXPRESS

wire cavity. In general, the total emission rate depends on the mode density for a given wavelength, and also on the vacuum electric field strength at the specific location of the active region [24]. As seen from Fig. 2, the SE rate that couples into the tracked three lasing modes greatly altered as the axial location of the active region moves away from the original point. In an optical cavity, the SE rate is controlled by the local density of optical states (LDOS), which describes the available optical eigenmodes for photons at a specific position, orientation, and frequency. The LDOS for a dipole emitter oriented along a radial direction in a MNW cavity can be determined by the relation [25]:

$$\rho = \frac{\omega^2 n}{3\pi^2 c^3} + \frac{1}{2\pi^2 \omega} \mathrm{Im}\left\{\frac{E_{scat}}{D}\right\}. \tag{3}$$

where c is the speed of light in vacuum, ω is the frequency, n is the refractive index of the active semiconductor, D is the dipole strength, and E_{scat} is the contribution to the electric field due to scattering at the interfaces, evaluated at the position of the emitter. When dipole sources are placed in a MNW, the SE is treated as being emitted into spherical waves, a fraction of which become counter-propagating wavepackets in the cavity. The dipole strength D and E_{scat} are considered to be affected by the interference in the radiated field for all directions. While in the longitudinal direction, the wavepacket emitted to the left and reflected back by the smooth end facet will interfere with the wavepacket emitted to the right. If the interference between these two wavepackets is constructive, enhanced SE rate in the cavity is expected. Changing the axial location of the active region directly leads to the variation of the field interference between the dipole sources and two end facets of the MNW and therefore modifies the dipole strength D as well as E_{scat}, consequently altering the LDOS and the SE rate. Furthermore, periodic modulations of the SE rate can also be observed from Fig. 2, which, on the other hand, confirm that the field interference of the initially oppositely propagating wavepackets in the longitudinal direction dominantly contributes to the variation of the guided SE rate when the position of the active region changes.

In the absence of a cavity, our simulation demonstrates that only about 0.1% of the total SE rate can couple into the guided modes. While as seen from Fig. 2, a significant amount of the radiation from the radiating dipoles can couple into the guided modes in a GaN MNW, which is attributed to the high index of refraction of the MNW material compared to that of the ambience. The modifications of the guided SE rates at different wavelengths have different amplitudes and phases due to the dephasing process as the active region moves from the origin. For the active region placed 5.5 μm away from the original point (as indicated by the red dashed line in Fig. 2), the SE rate couples into the lasing mode at 367.7 nm (shown by the green line) is significantly enhanced and reach a value of 33.2%. However, the guided SE rates at 366 nm (shown by the red line) and at 364.3 nm (shown by the blue line) are about 15.8%, less than half the SE rate couples into the lasing mode at 367.7 nm. A different pattern is indicated by the grey dashed line in Fig. 2, where the active region locates 14.5 μm away from the original point. The guided SE rates couples into the lasing mode at 367.7 nm, 366 nm and 364.3 nm are 17.9%, 18.7%, 19.5%, respectively, which are comparable to each other. We have presented that the guided SE rate, which is strongly affected by the electric field pattern distribution, is location-dependent and that of different modes differ from each other even under the same excitation condition. This fact is crucial in studying the laser output behavior in F-P lasers.

In view of these results, it can be seen that the position of the active region plays a key role in determining the lasing mode of MNW lasers. Therefore, we propose that cavity controlled emission for an F-P MNW laser can be realized due to the location-dependent field distribution, and we call it “self-selection mechanism of Fabry-Pérot mico/nanoscale wire cavity for single-mode lasing”; i.e., in the experiments on laser excitation, when the excitation source is placed at the position where the guide SE rates of several resonant modes are

Optics EXPRESS

comparable, multiple F-P modes will be observed. However, if the pump source is paced at the position where the guided SE rate of a single resonant mode is significantly enhanced while that of the other modes are inhibited or slightly enhanced, single-frequency lasing will be generated from the MNW laser.

4. Experimental methods

To experimentally investigate the cavity controlled emission from MNWs, we have fabricated and characterized GaN MNW lasers. Here the GaN MNWs were synthesized on sapphire substrates by Thomas Swan CCS- Metal Organic Chemical Vapor Deposition (MOCVD) system. Before growth, the substrate was heated to 1100 °C for 20 minutes under atmosphere of ammonia. Then GaN MNWs were grown at 1000 °C at a pressure of 200 Torr. Trimethylgallium (TMGa) and ammonia (NH_3) were used as the precursors in the growth. The TMGa flow rate was maintained at 78 μmol min-1 (15 sccm) and the NH_3 flow rate was kept at 223.21 mmol min-1 (5 slm). Pure hydrogen (H_2) was used as the carrier gas.

The room-temperature photoluminescence (PL) was inspected under the excitation of a He-Cd laser. The third harmonic (355 nm) of a Nd:YAG laser (1 kHz, 1 ns pulse width) was used as the excitation source. The type of the spectrometer is Andor/SR-500i-D1-R, with a resolution of 0.08 nm. Before measurements, some wires were removed from the growth substrate and dispersed on a piece of sapphire wafer. The laser beam was focused on individual wires at different positions along the MNW's axial length by a microscopic objective lens to a spot of ~16.7 μm in diameter, and the PL emission was collected by a photomultiplier tube in the UV–visible range.

5. Experimental results and discussion

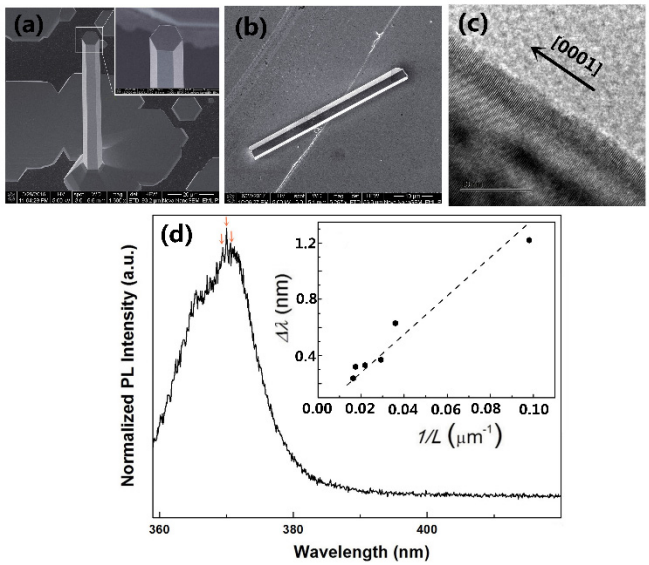

Fig. 3. (a) The SEM image of a single GaN MNW. (b) The SEM of a GaN MNW transferred to a sapphire substrate (c) The TEM micrograph of an individual GaN MNW. (d) Spontaneous emission of a 45-μm-long, 1.8-μm-diameter GaN MNW below lasing threshold at room temperature under a power density of 452 kW/cm^2. Arrows highlight three adjacent Fabry-Pérot peaks. Inset: Mode spacing vs inverse MNW length.

A typical scanning electron microscope (SEM) image of the MNW is displayed in Fig. 3(a), showing that the MNWs have sharp cleaved end facets, with a hexagonal cross section. Figure 3(b) shows the SEM of a GaN MNW transferred to a sapphire substrate, indicating both facets of the MNW are flat and smooth. Transmission electron microscopy (TEM)

Optics EXPRESS

examinations demonstrate that the MNWs are high-quality single crystal with growth along the [0001] direction (Fig. 3(c)). The uniform thickness and smooth surface morphology of MNWs are important for waveguiding without large losses from surface emission. Figure 1(a) shows the PL spectrum of a 35-μm-long, 1.2-μm-diameter GaN MNW with a narrow peak at around 366 nm and a full width at half maximum (FWHM) of 15 nm, corresponding to the typical near-band-edge emission of GaN. Below the lasing threshold, pronounced Fabry-Pérot oscillations (red arrows, Fig. 3(d)) can be resolved over a broad band-edge emission band of GaN wires, suggesting the observation of the longitudinal cavity modes resonated between two MNW-end facets. The emission spectra obtained from different MNWs show a pronounced modulation over a wide spectral range with the modulation period inversely proportional to MNW length (inset, Fig. 3(d)), demonstrating that the MNW functions as an optical F–P resonator along its axial length.

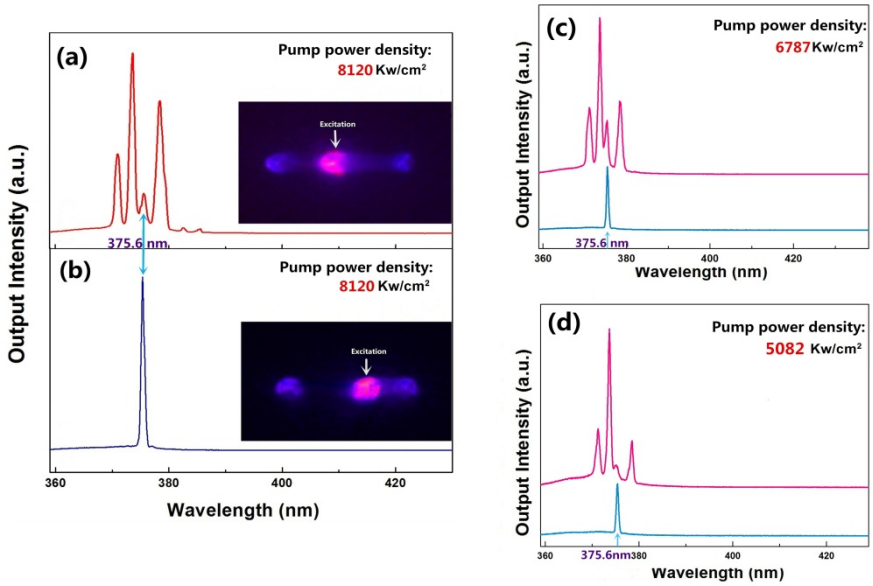

Fig. 4. The laser spectrum of a single 61-μm-long, 2.15-μm-diameter GaN MNW pumped well above the lasing threshold at room temperature under a power density of 8120 kW/cm^2: (a) when the excitation light spot is placed at a distance of 27.8 μm from the left end face of the MNW. The inset is the corresponding CCD image of the MNW; and (b) when the center position of the excitation light spot is placed at a distance of 39.7 μm from the left end face. The inset is the corresponding CCD image of the MNW. Output spectra of the MNW pumped well above the lasing threshold at room temperature under a power density of (c) 6787 kW/cm^2 and (d) 5082 kW/cm^2. The upper red line represents the output spectra with the same excitation position as (a) indicates; the lower blue line represents the output spectra with the same excitation position as (b) indicates.

Optics EXPRESS

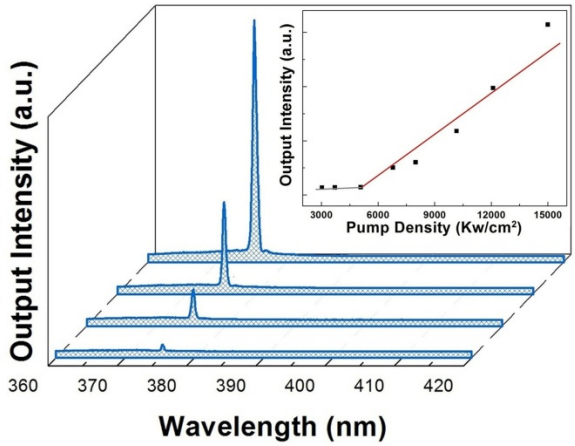

Fig. 5. Output spectra of the MNW show clean single-wavelength lasing at different excitation intensities. The inset is output intensity vs pump power density measured for lasing peak at 375.6 nm.

Lasing spectra of a single 61-μm-long, 2.15-μm-diameter GaN MNW are performed in the following research. When the excitation light spot is placed at a distance of 27.8 μm from the left end facet of the 61-μm-long, 2.15-μm-diameter MNW, laser spectrum is demonstrated in Fig. 4(a), and the inset is the corresponding charge-coupled device (CCD) image of optical emission from the GaN MNW. As shown in Fig. 4(a), when the MNW is pumped well above the lasing threshold, multi-mode lasing spectra are observed. Besides, the CCD images of the MNW (the insets in Figs. 4(a) and 4(b)) at high pump density show significant on-axis emission appearing as two bright spots at the ends of the wire, also indicative of the longitudinal axial F–P lasing. With the use of Eq. (2), four remarkable peaks at 371, 373.6, 375.6 and 378.5 nm in Fig. 4(a) can be calculated assuming top-bottom F-P oscillations with the corresponding mode numbers to be 870, 861, 854 and 844 respectively. However, when the distance between the excitation source and the left end facet of the MNW changes from 27.8 μm to 39.7 μm, the output laser mode exhibits an obvious change under the same pump power density which is demonstrated in Fig. 4(b) (the inset shows the corresponding CCD image of the emission). Single-frequency lasing has been generated from the MNW after adjusting the excitation position. The resonant mode at a wavelength of 375.6 nm as indicated by the blue arrow in Fig. 4(b) shows a single sharp peak with the lasing threshold of 2.5 MW/cm^2 (inset, Fig. 5) and a FWHM of 0.6 nm (limited by the spectral resolution of the detection system), offering a strong suppression of side modes. When we keep the excitation position unchanged and alter the pump power density (Figs. 4(c) and 4(d)), the transition from multiple-mode emission to single-mode emission of the MNW still remains the same. Furthermore, the MNW laser exhibits stable single-frequency operation over a large range of pump power densities above the threshold, as Fig. 5 shows.

Optics EXPRESS

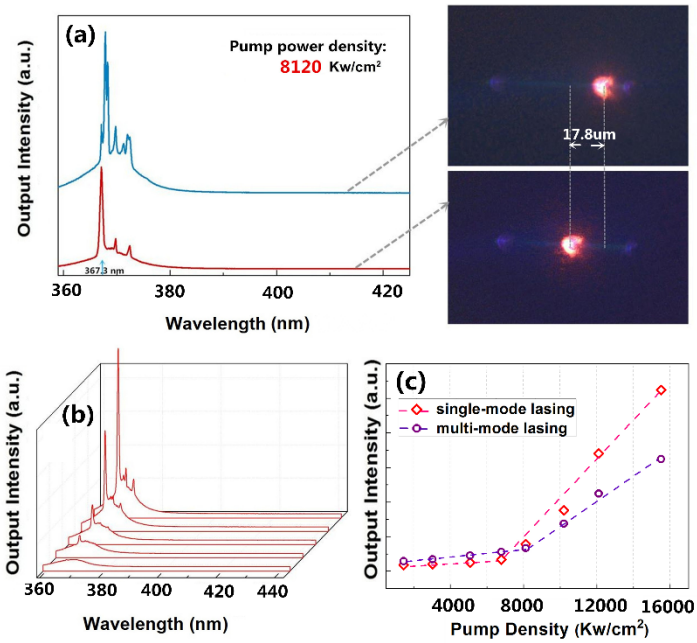

Fig. 6. (a) The laser spectrum of a single 72-μm-long, 2-μm-diameter GaN MNW pumped well above the lasing threshold at room temperature under a power density of 8120 kW/cm^2. The dashed-line arrows indicate the corresponding CCD images of the MNW with different excitation positions. (b) Output spectra of the MNW show clean single-wavelength lasing at different excitation intensities. (c) Power dependence for the peak wavelength (367.3 nm) of the 72-μm-long, 2-μm-diameter GaN MNW under single/multi-mode lasing.

Figure 6(a) shows the laser spectrum of a 72-μm-long, 2-μm-diameter GaN MNW pumped well above the lasing threshold. When the excitation light spot is placed at a distance of 11.8 μm from the right end facet of the MNW, multi-mode lasing is observed as the blue line shows. While when the excitation light spot moves 17.8 μm to the left facet of the MNW, single-frequency lasing is generated from the MNW under the same pump power density after adjusting the excitation position as the red line shows. Through controlling the excitation position, the 72-μm-long, 2-μm-diameter MNW laser exhibits stable single-frequency operation over a large range of pump power densities above the lasing threshold (Fig. 6(b)). Figure 6(c) indicates that the lasing thresholds of the peak wavelength under multi-mode lasing (8120 kW/cm^2) is higher than that under single-mode lasing (6787 kW/cm^2). The reduction of lasing threshold by optimizing the position of the active region, which is benefited from the greatly improved mode selection mechanism and avoiding excessive energy consumption in the mode competition, suggests a feasible approach to low-threshold MNW lasers.

Optics EXPRESS

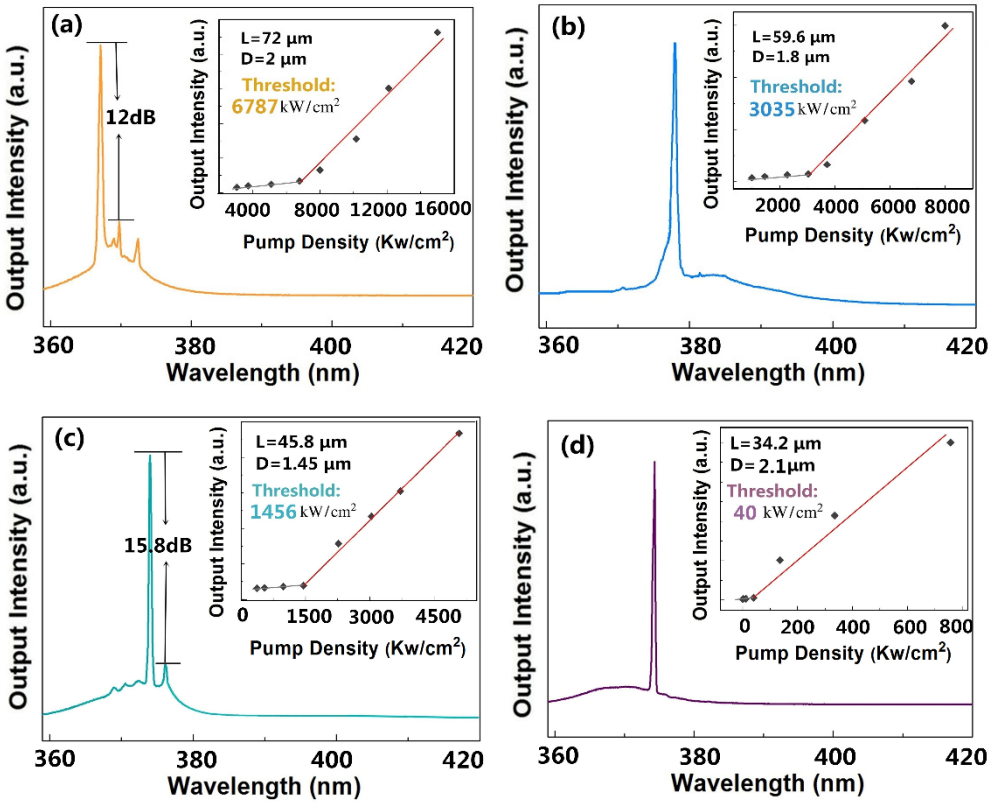

Fig. 7. Laser spectra of (a) a 72-μm-long, 2-μm-diameter MNW, (b) a 59.6-μm-long, 1.8-μm-diameter MNW, (c) a 45.8-μm-long, 1.45-μm-diameter MNW, (d) a 34.2-μm-long, 3.2-μm-diameter MNW lasers obtained well above the threshold at room temperature under a power density of (a) 8120 kW/cm^2 (b) 8120 kW/cm^2 (c) 5082 kW/cm^2 (d) 3034 kW/cm^2. The insets are output intensity vs pump power density measured for each lasing peak.

In addition to the field interference between the dipole sources and two end facets of the MNW, the change of the excitation power also affects the field distribution in a MNW. Because the field distribution is close related to the group index of the MNW, and the group index will change under different excitation power due to the changing of excited carrier concentrations [26, 27]. However, we have observed and compared the transition from multiple-mode emission to single-mode emission of the MNWs under the same condition of the pump power density (Figs. 4(a)-4(d), Fig. 6(a)), and changing the pump power density has no impact on the single-mode lasing of the MNWs (Fig. 5, Fig. 6(b)). Therefore, the change of the excitation power is not a cause for the transition to the single-mode emission of the MNWs. Combining the experimental results with the previous simulation prediction, conclusions can be made that the position of the active region plays a key role in determining the lasing mode of MNW lasers. The location-dependent field distribution in MNWs can be used for mode selection, which selects only one dominant mode and suppresses other individual resonant modes within the lasing range due to the interference between the wavepackets reflected by the two end-facet mirrors, fully proving the self-selection mechanism of Fabry-Pérot micro/nanoscale wire cavity for single-mode lasing. Furthermore, the reproducibility of single-mode operation in MNWs has been verified in other MNWs with different diameters and lengths by means of adjusting the position of the excitation source via making use of the self-selection mechanism of the Fabry-Pérot cavity. For illustrative purposes, laser spectra of four single-mode MNW lasers are shown in Figs. 7(a)-7(d). For the

Optics EXPRESS

45.8-μm-long, 1.45-μm-diameter MNW laser (Fig. 7(c)), side-mode suppression ratio (SMSR) is calculated to be 15.8 dB obtained at pump intensity well above the threshold. While the 59.6-μm-long (Fig. 7(b)) and the 34.2-μm-long (Fig. 7(d)) MNW lasers show better monochromaticity with single sharp peaks. The estimated quality factor of these GaN MNWs is about 730 ~937, indicating high crystalline quality of the MNWs with smooth end facets. As seen from Fig. 7, with the length of the MNW decreases from 72 μm to 34.2 μm, the lasing threshold dramatically decreases from a value of 6787 kW/cm^2 to a minimum of 40 kW/cm^2. Since the gain region of each MNW laser remains unchanged due to the fixed excitation light spot diameter, decreasing the length of the MNW decreases the length of the absorption region (the region of the MNW without excitation) of the semiconductor MNW. Therefore, with reduced re-absorption of the light emission by the semiconductor material, the threshold decreases with decrease in the length of the MNW. Therefore, the single-frequency low-threshold lasing can be achieved in MNWs with appropriate length comparable to or less than 35 μm.

6. Summary

In conclusion, we have demonstrated stable, single-frequency output from single laser that consists of a linear, double-facet GaN micro/nanoscale wire functioning as gain medium and optical resonator. We have found and proved that the position of the active region plays a key role in determining the lasing mode of MNW lasers, which can be used to realize single-mode lasing in MNWs. Self-selection mechanism of Fabry-Pérot micro/nanoscale wire cavity for single-mode lasing has been fully proved due to the location-dependent field distribution in MNWs, which in this letter is characterized by suppressing the multiple longitude mode oscillation of the MNW lasers. The single-mode low-threshold lasing action demonstrated here in GaN MNWs is suitable for miniaturization of simple manipulation, which opens an opportunity to realize the practical applications of the MNW lasers and meet the goal of easy integration in constructing micro/nanoscale photonic and optoelectronic circuits and devices.

Funding

The National Natural Science Foundation of China (Grant No. 61334005 and 11505015); the Key National Research and Development Program (Grant No.2016YFB0401801 and 2017YFB0405000); Science Challenge Project (JCKY2016212A503); Beijing Municipal Science and Technology Project (Z161100002116037).

Acknowledgments

The authors would like to thank all the staff during the measurements at the beamline 1W1A at BSRF.